Fault Distribution, Slip-rate Determination, and a Focused Seismicity Study of the Pyramid Lake Basin

NEHRP grant G12AP20110 (IMW)

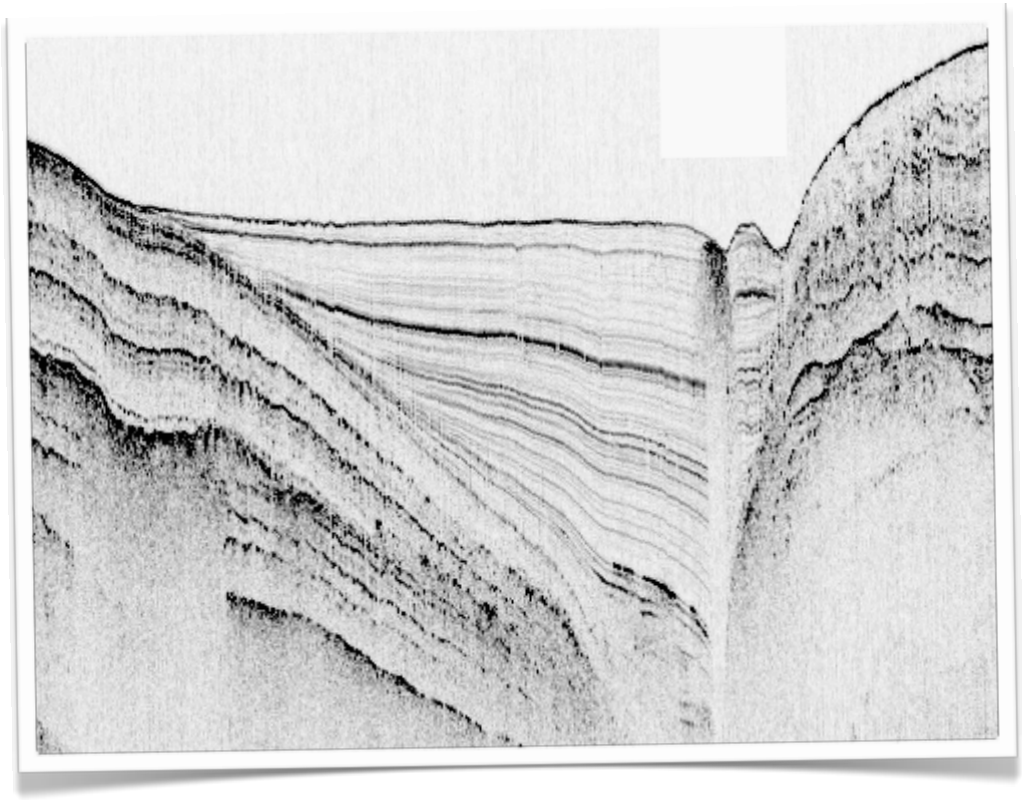

Graham Kent Nevada Seismological Laboratory/0174
University of Nevada, Reno, Reno NV 89557

June 1, 2012 – December 31, 2013

Executive Summary: A seismic CHIRP survey of Pyramid Lake, Nevada reveals a long-term history of fault motion within a key sector of the northern Walker Lane. High resolution (decimeter) sub-surface imagery, together with dated piston and gravity cores, were used to produce the first complete fault map beneath the lake. This approach enabled the determination of vertical slip-rates for the major fault zones. The more than 500 line-kilometers of CHIRP data imaged complex fault patterns throughout the Pyramid Lake basin. Fault architecture beneath Pyramid Lake reveals a reversal of fault polarity, where down-to-the east patterns of slip on the dextral Pyramid Lake fault to the south give way to down-to-the-west geometries to the north within a mostly extensional environment (i.e., Lake Range fault). The Lake Range fault predominantly controls extensional deformation within the northern two-thirds of the basin, and exhibits varying degrees of asymmetric tilting and divergence due to along-strike segmentation. This structural configuration likely results from a combination of changes in slip-rate along strike and the splaying of fault segments onshore. The potential splaying of fault segments onshore tends to move the focus of extension away from the lake. The combination of normal and oblique-slip faults in the northern basin gives Pyramid Lake its distinctive "fanning open to the north" geometry. The dense network of oblique-slip faults in the northwestern region of the lake are short and discontinuous in nature, possibly representing a nascent shear zone. In contrast, the Lake Range fault is long and well defined. Preliminary vertical slip-rates measured across the Lake Range and other faults provide new estimates on extension across the Pyramid Lake basin. A minimum vertical slip rate of ~1.0 mm/yr is estimated along the Lake Range fault. When combined with fault length, slip rates yield a potential earthquake magnitude range between M6.4 and M7.0. A rapid influx of sediment shortly after the end of the Tioga glaciation, between 12.5 ka to 9.5 ka, records little to no slip on the Lake Range fault. In contrast, the basin has experienced a decrease in sedimentation rate for the past 9.5 ka, but an escalation in earthquake activity on the Lake Range fault. CHIRP imagery show potential for 3 or 4 major earthquakes assuming a characteristic offset of 2.5 m per event. Regionally, our CHIRP investigation helps to reveal how strain is partitioned along the boundary between the northeastern edge of the Walker Lane and the northwest Basin and Range proper. *The original proposal also had an element of micro-seismicity studies, but the panel requested that the reduced budget be solely focused on the CHIRP work.*

Introduction and Rationale: Dextral shear is unevenly distributed along the western margin of North America with ~75-80% of the Pacific and North American plate motion being accommodated by the San Andreas fault system in the west. The remaining deformation occurs eastward toward the Basin and Range province (Atwater, 1970, Atwater and Stock, 1998, McQuarrie and Wernicke, 2005). The structurally complex transition between the Sierra Nevada microplate and the Basin and Range, known as the Walker Lane Deformation Belt to the north

and the Eastern California Shear Zone to the south, is identified through seismic, geodetic, and geologic data (Stewart 1988; Dokka and Travis, 1990; Argus and Gordon, 1991; Thatcher et al., 1999; Svarc et al., 2002; Bennett et al., 2003; Unruh et al., 2003; Oldow, 2003; Hammond and Thatcher, 2004; Wesnousky, 2005a,b,c). This approximately 100-km-wide belt of seismicity and active faulting accommodates ~20% of relative motion between the Sierra Nevada microplate and stable North America (Thatcher et al., 1999; Thatcher et al., 2003; Bennett et al., 2003; Hammond et al., 2011). Studies show that most of the deformation in the Walker Lane occurs at the eastern and western margins of the belt (Hammond et al., 2011). Furthermore, seismicity is concentrated at the eastern and western boundaries of the Basin and Range, with higher rates of strain localized on the western side within the central Nevada seismic belt and the Walker Lane (Eddington et al., 1987).

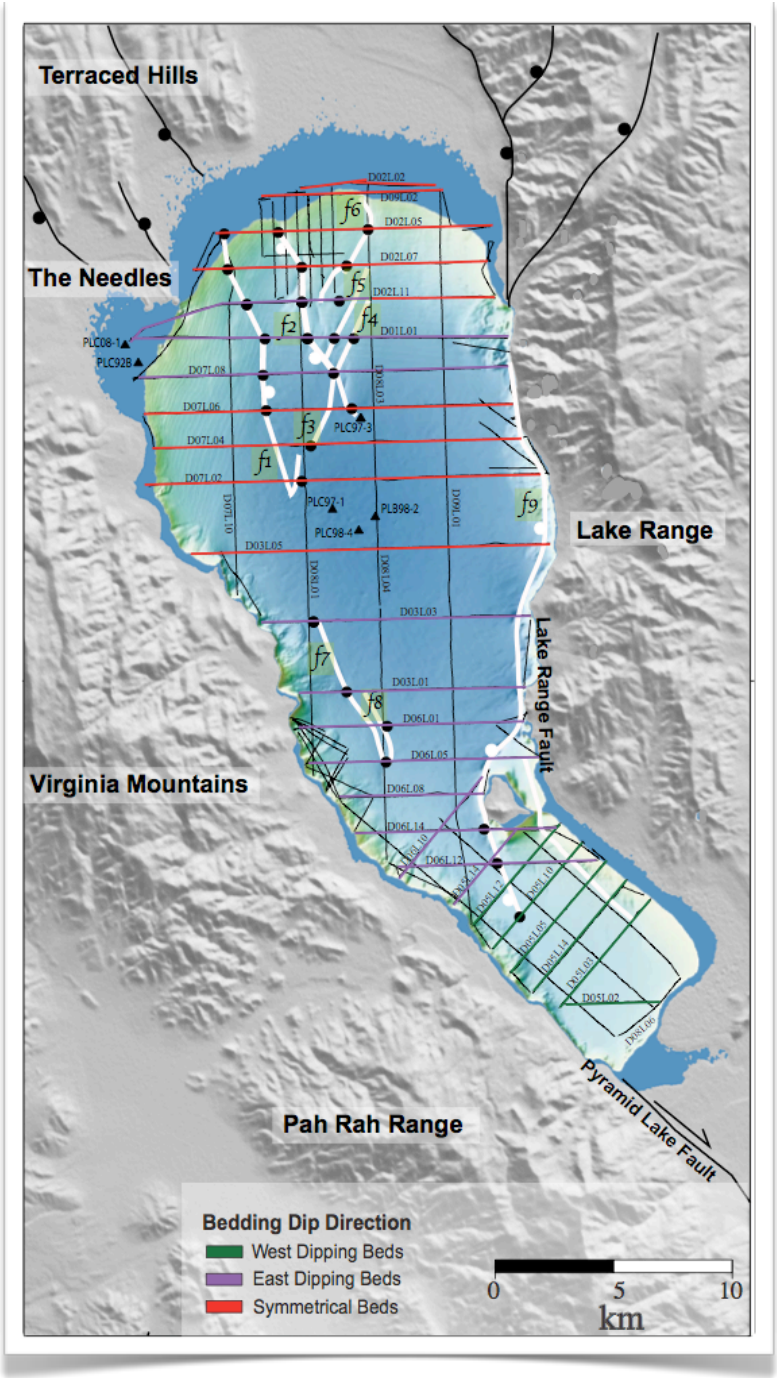

Figure 1 Map of Pyramid Lake, Nevada located ~64 km northeast of Reno, Nevada. The green, purple, red and light black lines within the lake are the CHIRP survey lines with the green lines indicating a regional west dip, purple lines designate east-dipping reflectors, red portray symmetrical horizons, and light black lines are the remaining CHIRP survey lines. The thick white lines are significant faults mapped from CHIRP profiles. The triangles are sediment cores collected by Mensing et al. (2004), Benson et al. (2002) and Benson et al. (2013). The black circles are locations of slip-rates calculated within the lake.

Pyramid Lake is located toward the eastern margin of the northern Walker Lane in a transitional zone between two distinct geological regions: the Walker Lane Deformation Belt and the Basin and Range province. Within the northern Walker Lane, Pyramid Lake is located in a key region where transtension is accommodated through a series of mainly dextral strike-slip faults (Turner et al., 2008). Northwest of Pyramid Lake (e.g., Honey Lake fault zone) dextral faults strike northwest, while a geometry of north-striking normal fault bounded basins (e.g., Lake Tahoe basin, Dingler et al., 2009) dominates toward the southwest. South of Pyramid Lake, within the Carson domain (Stewart, 1988), a more complex pattern of deformation is observed, characterized by significant amounts (> 30°) of clockwise vertical-axis rotation bounded by ENE-striking sinistral faults (Cashman and Fontaine, 2000).

Pyramid Lake is the remnant of the Pleistocene lakes that once covered much of the Great Basin. During the late Pleistocene, the closed valleys in the Great Basin contained a series of large lakes. The two largest of these lakes were Lake Bonneville and Lake Lahontan (Gilbert, 1890; Adams et al., 1999). At its highstand, Lake Lahontan straddled the boundary between the Walker Lane and the central Basin and Range province (Adams et al., 1999). The deepest point of ancient Lake Lahontan is within the present-day Pyramid Lake basin (Benson and Mifflin, 1986).

The lake-bed stratigraphy of Pyramid Lake provides a detailed record of the geologic and tectonic history of the basin. The low wave energy of the hydrologic system preserves the stratigraphy and chronicles the tectonic deformation (e.g., Kent et al., 2005; Dong et al., 2014). The asymmetric (i.e., half-graben) geometry creates low-lying topography, which records and preserves the deformation. Remnant sections of ancient Lake Lahontan (i.e., Pyramid Lake) provide ideal opportunities to investigate the rapidly deforming northern Walker Lane (Adams et al., 1999; Thatcher et al., 1999). Many remnant sections of Lake Lahontan have been targets for extensive paleoclimate studies including cores used for chronostratigraphic analysis. Cores collected from Pyramid Lake highlight a nearly continuous record of sedimentation extending to 48 ka (Benson et al., 2013).

The Pyramid Lake basin provides an ideal natural laboratory to study transtensional deformation in the Northern Walker Lane. In June 2010, the University of Nevada, Reno, Scripps Institution of Oceanography, and the United States Geological Survey collected more than 500 line-kilometers of decimeter resolution seismic imagery in Pyramid Lake, Nevada (Fig. 1). The Compressed High Intensity Radar Pulse (CHIRP) seismic system produces images beneath the lake to ~70 m depth, allowing the mapping of faults and measurement of stratigraphic offsets. These features unravel the structural evolution of the complex Pyramid Lake basin. Five dated

sediment cores from previous paleoclimate investigations (Mensing et al., 2004; Benson et al., 2002, Benson et al., 2013) provided a chronostratigraphic framework for our dense network of CHIRP profiles beneath the lake.

In this follow-on study (acquisition was funded through the *Bureau of Indian Affairs*), CHIRP imagery is critical in the production of the first comprehensive fault map of the Pyramid Lake region. Fault locations are refined and then correlated to mapped faults on land. The stratigraphic offset and sense of dip across faults observed on CHIRP records were documented and compared to displacements observed on adjacent profiles in order to map fault trace locations. The resulting fault map not only contributes to understanding strain partitioning in this basin but also in classifying earthquake hazards for nearby metropolitan areas around the lake (e.g., Reno and Sparks, Nevada). Furthermore, a suite of piston and gravity cores (Benson et al., 2013) helped to calculate sedimentation rates, placing important constraints on slip rates and earthquake timing calculations for faults beneath the lake. Here we present new interpretations that reveal the style of deformation in the basin, and together with age control, yield slip rate estimates for the faults in Pyramid Lake.

Results: The results from the numerous CHIRP profiles catalogue the structural regime of the Pyramid Lake basin. Stratigraphic patterns observed in the profiles give an understanding of the fault architecture beneath the lake. The stratigraphy also allows identification of a cluster of earthquake events in the Holocene. By correlating stratigraphic layers to sediment cores, vertical slip rates (Table 1) can be calculated across faults. Understanding the rates of motion on these large, active fault systems has implications to earthquake hazards for northern Nevada and the Reno metropolitan area.

Polarity Flip and Fault Segmentation in Pyramid Lake

One of the most prominent features observed in the CHIRP profiles is an alternating pattern of dip directions within the sedimentary layers (Figures 2&3) . Most notably, the stratigraphy highlights a flip in basin polarity near Anaho Island. Sediment layers tilt and thicken toward normal faults, similar to what is imaged in other extensional settings (Bosworth, 1985; Flannery, 1990; Rosendahl et al., 1992; Driscoll et al., 1995, Brothers et al., 2009; Kell et al., submitted). The alternating dips show where fault motion dies on one fault and steps to another by highlighting the changes in fault polarity.

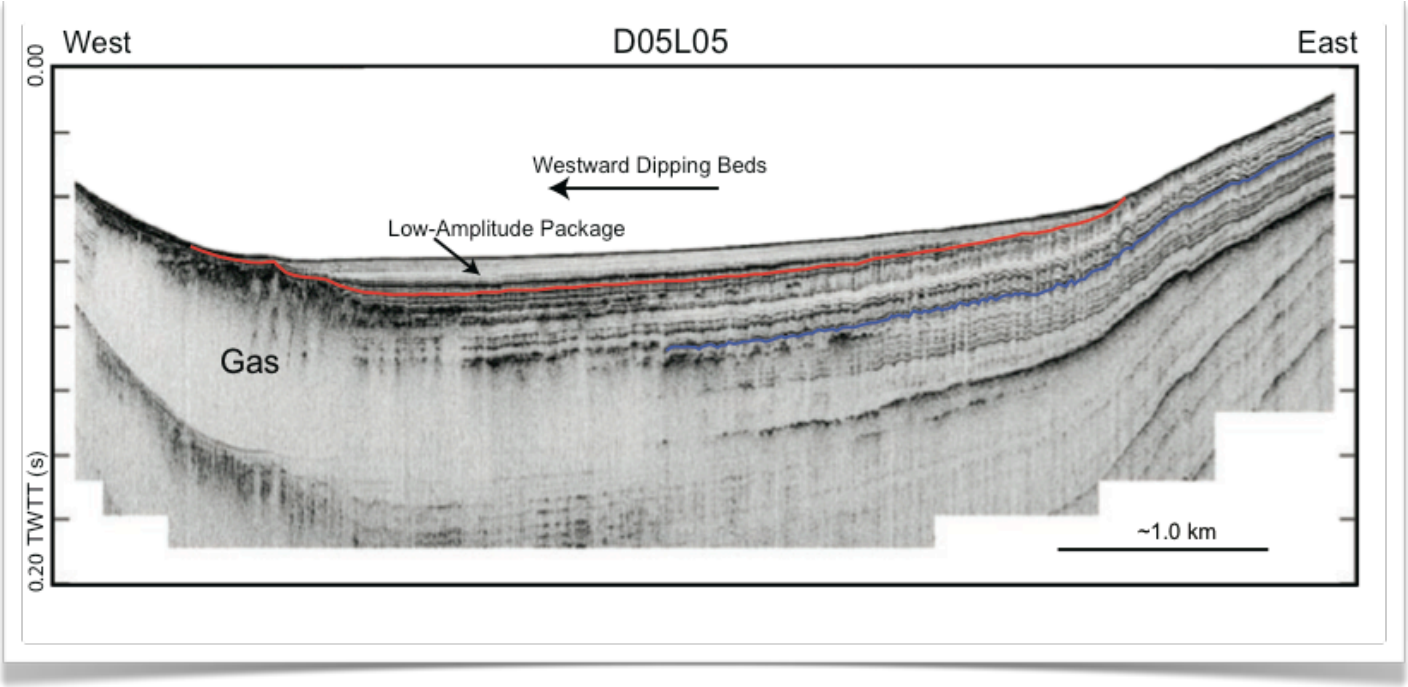

Figure 2 CHIRP Line D05L05 (for location see Figure 1) is an east-west oriented profile showing a regional westward dip as well as gas wipeout in the west and the low amplitude sediment package above the red horizon. The red and blue horizons correlate to core PLC92B tracked from Line D07L08 giving ages of ~14 ka and ~48 ka, respectively.

Results indicate that the Pyramid Lake fault enters the basin along the southwestern shoreline of the lake (along the panhandle). The fault is neither directly seen in the CHIRP profiles nor observed onland through geological mapping. By defining the western shore, there is no surface expression to be mapped, and CHIRP profiles were not able to cross the fault trace to image the fault directly. Insight about the location and the sense of motion on the Pyramid Lake fault can be gained from the four southernmost profiles that run perpendicular to the southwestern shore. These profiles display a regional southwestward dip (divergence) in stratigraphy (e.g., Fig. 2). This divergent pattern suggests that the Pyramid Lake fault has some northeast-dipping, normal component near its northern termination. The fault slip changes to oblique motion as it ends and transfers strain (steps-over) onto the Lake Range fault. Oblique motion on the Pyramid Lake fault would help to form the "hole" which is the southern basin/ panhandle. The impact that this motion has on the morphology of the lake bottom gives strong evidence that the fault extends along the western shoreline of the panhandle.

Farther north, profiles (e.g., Fig. 3, D06L12) reveal the transfer of motion onto the Lake Range fault. The stratigraphic pattern changes to a regional eastward dip near Anaho Island. The transition between the northern termination of the Pyramid Lake fault and the beginning of the

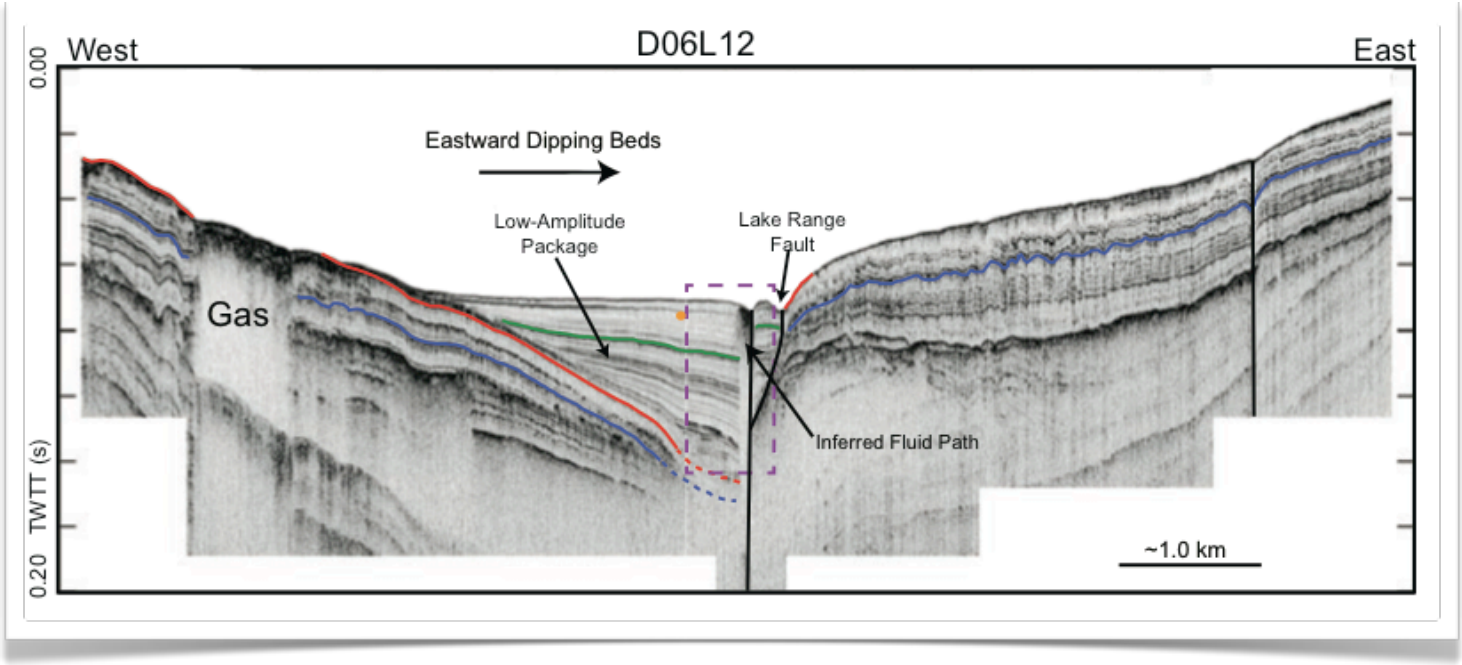

Figure 3 CHIRP Line D06L12 (for location see Figure 1) shows the Lake Range fault and the low amplitude sediment package infill to the west. It shows distinct eastward dipping sediment layers. The orange dot is where core PLC97-1 is traced from the intersection of Line D03L05 and Line D06L12. The orange dot correlates to core PLC97-1 tracked south to Line D06L12. The green horizon is where the offset was measured as well as the extrapolated dates from core PLC97-1. The red and blue horizons correlate to core PLC92B mapped from Line D07L08 giving ages of ~14 ka and ~48 ka, respectively.

Lake Range fault is seen between line D05L12 and line D05L14 (locations shown in Fig. 1). Between the two profiles the stratigraphic horizons change from a western dip to an eastern dip. The Lake Range fault dominates the architecture of the basin north of Anaho Island and controls stratigraphic patterns along the eastern shoreline (Fig. 1).

The pattern of regional eastern dip oscillates into segments that are more symmetric (these regions are color-coded in Fig. 1. This change between symmetrical and asymmetrical architecture provides evidence for fault segmentation along the Lake Range fault. Slip on the Lake Range fault dominates in regions that have a strong eastward dip. These regions show where the stratigraphic horizons tilt and thicken into an extensional, west-dipping fault zone (Fig. 4). Regions with more symmetric horizons (i.e., Fig. 5) show where strain is not focused or decreases on the Lake Range fault. There are two options to explain this alternating pattern of symmetry/asymmetry. One explanation invokes strong segmentation along the strike of the Lake Range fault with splays that occasionally trend onshore, north to northeast striking, away from the main trace. In this mode, slip is somewhat constant along strike, but dip is controlled by relative distance of the fault from the shoreline. Otherwise, fault segmentation may genuinely represent strong gradients in slip along the fault trace, with little or no “horse-tailing” onshore.

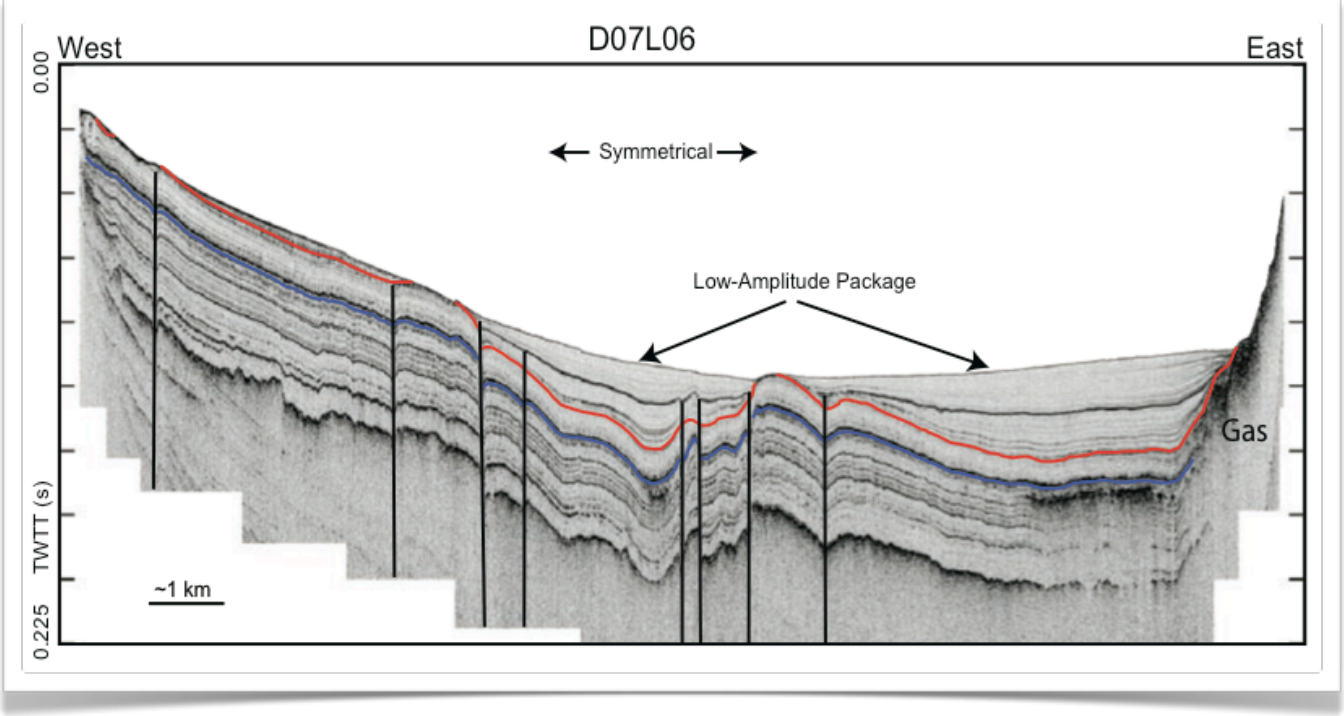

Figure 4 CHIRP profile of Line D07L06 (for location see Figure 1) shows asymmetrical beds as well as the onset of the northwest fault network. The low-amplitude package is thick on this line, gas is present to the east, and the Lake Range fault is not apparent in the profile. The red and blue horizons correlate to core PLC92B tracked from Line D07L08 giving ages of ~14 ka and ~48 ka, respectively.

In reality, it may be a hybrid model where segmentation is supported through onshore splays, but also by changes in cumulative offset along-strike.

The change in deformation style from the south to the north is evidence of both an architectural change in basin polarity, and strong segmentation of the Lake Range fault. Broadly speaking, sediment layers south of Anaho Island dip west (or southwest) while layers north of the island dip towards the east. This change in deformation corresponds to a change in basin geometry. South of Anaho Island (i.e., the panhandle) the basin is narrow and northwest-oriented while north of the island the basin fans open or widens and trends north-south. This latter pattern reflects a combination of the north-striking Lake Range fault and a series of northeast-striking oblique slip faults.

Pyramid Lake fault patterns

Predominantly transtensional faulting is observed in CHIRP data in the northwest end of the Pyramid Lake basin near the Needles (Fig. 6). The northwest sector of the basin has its own unique deformation style. The density of oblique-slip faults markedly increases to the northwest. In contrast the overall length of these faults decreases. The Lake Range fault continues for >20 km along the eastern shoreline of the lake. The faults in the northwest are 2-10 km long, barely

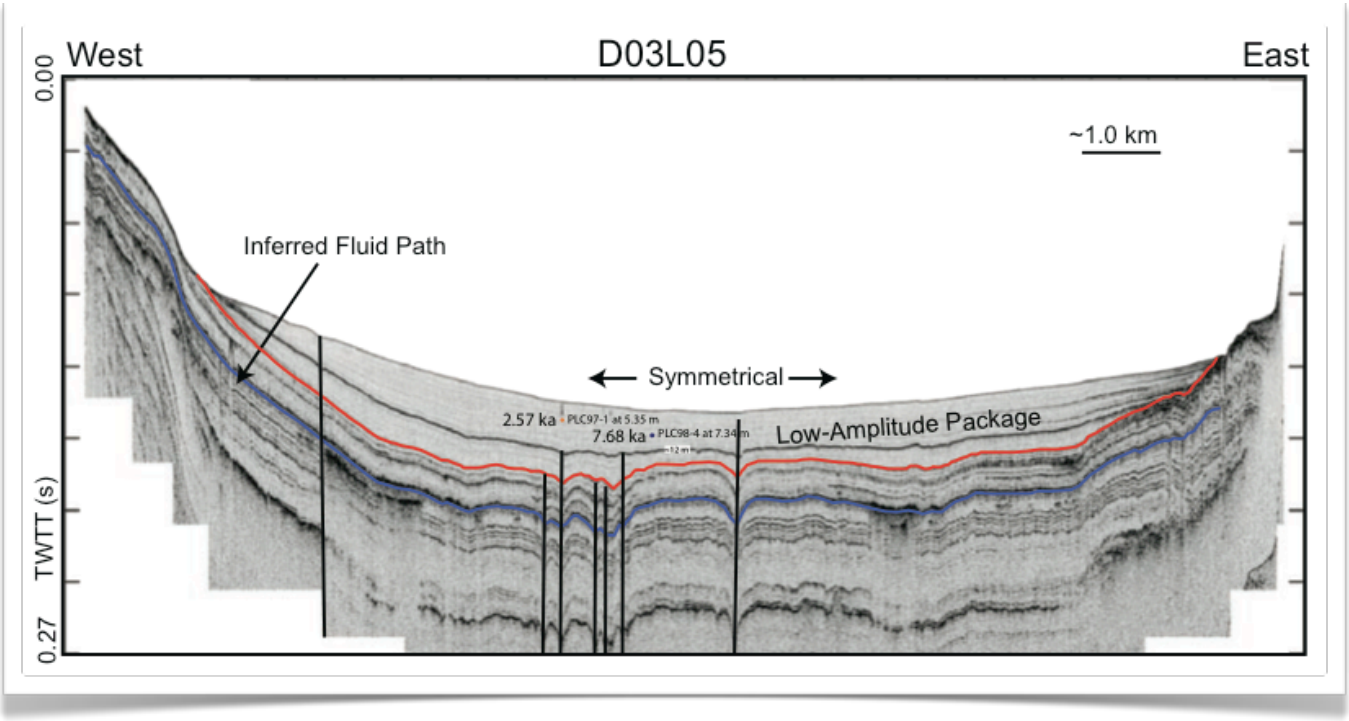

Figure 5 CHIRP profile of Line D03L05 (for location see Figure 1) shows symmetrical beds. It is unclear if the east edge of the profile is the Lake Range fault or the side of the basin yet numerous other dip-slip faults are present throughout the profile. Gas wipeout and an inferred fluid path are also observed. The red and blue horizons correlate to core PLC92B tracked from Line D07L08 giving ages of ~14 ka and ~48 ka, respectively.

crossing two east-west oriented CHIRP lines. These short, segmented faults are very suggestive of a developing shear zone (Faulds et al., 2005, Wesnousky, 2005a).

The faults imaged in the 2D profiles show signatures of strike-slip deformation in addition to their obvious vertical offsets. Strike-slips faults are identified in seismic stratigraphy though a signature "V" where layers dip in toward a fault plane. This signature is due to small amounts of extension on the fault plane that allow the sediment layers to continually dip toward the fault. The significant faults documented in the northwest edge of the basin are likely north- to northwest-striking oblique faults and northeast striking oblique slip faults. The transtensional faulting in the northwest end of the basin forms the "fan" shape of the northern basin (Fig. 1). Unlike the more mature Lake Range fault and Pyramid Lake fault, the shorter faults imply that the northern basin is an immature system that has yet to coalesced into a single continuous fault.

Stratigraphy and cores

By correlating the stratigraphy observed in the high resolution CHIRP data with core data from Mensing et al. (2004), Benson et al. (2002), and Benson et al. (2013) it is possible to resolve some of the vertical slip history within the basin. There is a depth-age distribution of sediments within Pyramid Lake attributed to the erosion and reworking/resuspension of older sediments

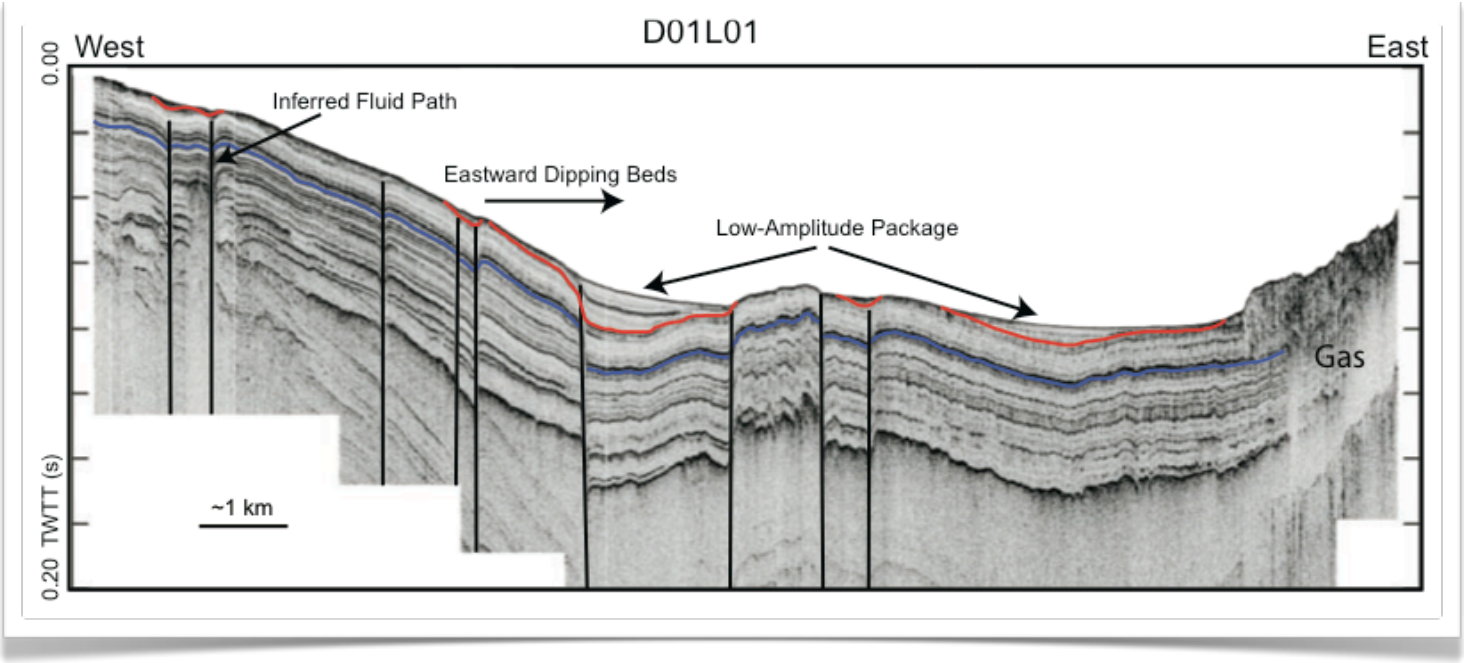

Figure 6 CHIRP Line D01L01 (for location see Figure 1) shows an increased number of faults toward the northwestern portion of the basin. There is also a noticeable eastward dip of the beds. The red and blue horizons correlate to core PLC92B tracked from Line D07L08 giving ages of ~14 ka and ~48 ka, respectively.

from the sides of the basin that was well known from coring before CHIRP profiles were collected. The ages of the sediments along the edges of the basin are much older than the deep, middle section of the lake (Benson et al., 2002). This age unconformity is imaged in the CHIRP data and highlights a depositional hiatus. The unconformity may reflect different styles of deposition: during periods of glaciation sediment may, on average, have been finer-grained and deposition was in a distal phase thereby producing a pattern of sedimentation that mimics topography. Holocene deposition consisted of much coarser material that bypassed the steepest slopes and only infilled in the deepest sections of the basin, mostly fed by the nearby Truckee river delta at the south end of the lake.

Using chronologic control from sediment cores and the high fidelity stratigraphic record observed in the CHIRP profiles, sediment layers can be tracked across the faults throughout the basin. Correlating the sediment ages with vertical offsets, allows (in some cases) the vertical slip rate (vertical throw rate) to be calculated across several of the more significant faults (Table 1). Core PLC92B was dated using GISP2age with the top dated at 13.9 ka and the bottom, at a depth of 17.325 m, showing an age of 47.9 ka (Benson et al., 2013). This core is located at the west end of Line D07L08 just to the north of the profile (Fig. 1). The horizons that bound the top and bottom of the core were correlated with the nearest stratigraphic horizon and then tracked south (using Fledermaus and Kingdom Suite) around the basin to the Lake Range fault on Line

Table 1. Distribution of Slip Rates on Significant faults within Pyramid Lake

Fault	Line	Slip Rate (mm/yr)
f1	D02L05	0.1
	D02L07	0.1
	D02L11	0.1
	D01L01	0.27
	D07L08	0.14
	D07L06	0.18
f2	D02L05	0.11
	D02L07	0.31
	D02L11	0.3
	D01L01	0.17
	D07L08	0.35
	D07L06	0.16
f3	D07L04	0.13
f4	D01L01	0.1
f5	D02L11	0.13
	D01L01	0.11
f6	D02L05	0.13
	D02L07	0.07
f7	D03L03	0.4
	D03L01	0.1
	D06L05	0.3
f8	D06L01	0.19
f9	D06L14	1.5
	D06L12	1
	D05L10	0.2

D06L12 to constrain the long-term slip rate and reconstruct the slip history.

Holocene Slip History of the Lake Range Fault on Line D06L12

The stratigraphic horizons that correlate with the top (13.9 ka) and bottom (47.9 ka) of the core in the northwest sector of the lake were tracked southward around the basin until reaching Line D06L12 (Fig. 3). These layers represent the layers recorded in core data that can be used to date CHIRP horizons. The blue horizon represents the bottom of the chronologically tied core horizon (47.9 ka) while the red horizon depicts the top (13.9 ka). The red horizon marks a change in deposition when the low-amplitude package began. Dates support that the low amplitude package is Holocene age and was deposited after the last glaciation (Tioga) around 12,500 years ago.

The long-term slip history of the Lake Range fault is not documented, but given the size of the fault escarpment and depth of the basin it has likely been active for the entire Pleistocene and perhaps well into the Pliocene. Near the southern terminus of the fault (Fig. 3), there was vertical displacement across the fault and an infilling of sediments into a low (~ 14 ka). After the red horizon was deposited (~14 ka), the Lake Range fault experienced modest thickening of sediments into the hanging wall near the fault. The thickening (showing vertical offset) is not resolvable to one or possibly numerous events. After the sediment infilling (and most likely correlated with melting glaciers in the Tahoe basin) many more stratigraphic horizons were

deposited into the existing low topography. Little to no differential slip is recorded across these concordant layers within this interval.

After the thick wedge of sediments was deposited, significant vertical offset on the Lake Range fault is recorded in the stratigraphy. This series of events allows for the quantitative amount of offset to be calculated, although per event slip can only be inferred. The orange dot in Figure 3 shows the bottom location of core PLC97-1, with an age date of 2.57 ka at 5.35m (Mensing et al., 2004) that correlates with the low-amplitude package in Line D06L12. The age of the green horizon was extrapolated from this core date in the center of the lake (Fig. 1) by assuming a constant sedimentation rate from the lakebed to the green horizon. This assumption gives an age of ~9.5 ka for the green horizon. The time difference between the green and red horizons (Fig. 3) provides a sedimentation rate of 0.17 cm/yr for the last 9,500 years. Published sedimentation rates of ~0.12-0.23 cm/yr for the past 7,630 years (Benson et al., 2002) correlate with this calculation.

Using the dated horizons from core PLC97-1 extrapolated to seismic profile horizons, dates were calculated for the red horizon to be 30.7 ka while core PLC92B placed the red horizon at 13.9 ka. The two different age calculations imply 16,000 years of "missing" sediment. This discrepancy of ages on the red horizon likely indicates a short interval of enhanced sedimentation that infilled the low topography during melting of Pleistocene glaciers. Sedimentation continued above the green horizon showing significant slip focused on the Lake Range fault A total of about 9 meters of stratigraphic offset have occurred since the deposition of the green horizon ~9.5 ka (3 to 4 events assuming a characteristic earthquake of 2-2.5 m of vertical throw). Layers above the green horizon cannot be reliably correlated across the Lake Range fault, making the 9.5 ka marker the last reference point for deformation.

Collapsing horizons in the seismic stratigraphy allows the measurement of growth on the fault system. Collapsing the low-amplitude package across the fault trace shows that most of the slip occurred after the deposition of the green horizon (i.e., in the last ~9.5 ka). Collapsing the green horizon shows little to no apparent offset below the green horizon. The minimal offset seen may be a horizon tracking error or it may be one small tectonic event. This observation means that all of the tracked horizons were before there was any significant vertical offset–thus all the slip has occurred since ~9.5 ka.

In summary, a heavy influx of sediment was deposited between 12,500 to 9,500 years ago due to end of Tioga glaciation. A drastic increase of high Sierra Nevada melt waters brought a surge of

sediment into the lake basin. During this time there was limited-to-no tectonic activity on the Lake Range fault. However, in the past 9,500 years, there has been reduced sediment deposition, yet significant offset on the Lake Range fault.

Lake Range fault slip rate

The recent slip rate calculated on the Lake Range fault along 3 profiles correlate with other Holocene slip rates in the northern Walker Lane. The age inferred for the green horizon (~9.5 ka) and the total offset seen across the fault (~9.5 m, Fig. 3) yields vertical Holocene slips rate between 0.2 and 1.5 mm/yr (Table 1). The West Tahoe and Stateline–North Tahoe faults have a normal slip rate of 0.7-0.8 and 0.60 mm/yr, respectively (Kent et al., 2005; Dingler et al., 2009). The Genoa fault has a reported Holocene slip rate of ~2-3 mm/yr, although longer-tern rates are closer to 1 mm/yr (Ramelli et al., 1999). Recent seismic work in Walker Lake constrains the slip on the Wassuk fault to be as much as 1.0 to 1.5 mm/yr over the past 20-30 k.y. (Dong et al., 2014). The ~1.0 mm/yr estimate on the Lake Range fault is consistent with a vertical slip rate of 0.609-1.096 mm/yr estimated by dePolo (1998).

The lower slip rate on the Lake Range fault occurs south of Anaho Island, overlapping where the Pyramid Lake fault is presumed to be active. A small distance to the north, where the Pyramid Lake fault has terminated, the slip rates on the Lake Range fault increase to ~1.5 mm/yr (Table 1). The fault scarp north of D06L12 (Fig. 3) used to calculate 1.0 mm/yr of vertical slip shows much greater offsets though horizons cannot be traced across the fault trace. These limitations indicate that observed rates are a minimum or underestimated rate for the length of the Lake Range fault. Thinning of stratigraphic units into the present-day fault location (Fig. 3) during the late Pleistocene (at the southern terminus of the Lake Range fault) also suggests that this section of the fault has recently lengthened southward. The lower rate at the very southern point of the fault supports that motion is extending to the south but has not been active for as long.

Given the proximity of the dates extrapolated from core PLC97-1 to the green horizon there is some potential that the reflector may be correlated to the Tsoyawata bed of the Mazama tephra, age dated at ~7.8 ka (Davis, 1978; Bacon, 1983). If true, the green horizon would then be a slightly younger age, giving a higher Holocene slip rate of ~1.2 mm/yr.

Additional slip rates

Additional Holocene slip rates were calculated throughout the lake (Table 1, black dots in Fig. 1) using offsets the 48 ka horizon. The calculations show the progression of slip rates along each of the significant faults in the basin. Though there is some variability along each fault, the rates

combine across the lake to show substantial vertical motion. These calculations range from 0.07 mm/yr to 0.4 mm/yr (Table 1). The rates are apparent vertical slip rates and possibly are inaccurate due to the obliquity between the fault trace and the profile but indicate that the Pyramid Lake basin is actively shearing due to the transtension of the northern Walker Lane. The "fanning open" of the northern basin is due to the interaction between the Lake Range normal fault, the dextral shear from the Pyramid Lake fault and others transtensional faults to the northwest.

Lake Range Fault Seismic Hazards

Many of the active Walker Lane and Basin and Range province normal faults have been studied through geological trenching and quantitatively calculated slip rates. The range-bounding normal fault of Smith Valley, Nevada has a clear ~3.5 m scarp in alluvium from one event, which gives a minimum and maximum slip rate of 0.125 mm/yr and 0.33 mm/yr, respectively (Wesnousky and Caffee, 2011). Through a compilation of various studies, the vertical component of coseismic offset of normal faults along the margins of the basins were found to vary from less than 1 m to greater than 4.5 m (Wesnousky et al., 2005a) resulting in an average offset of ~2.5 m.

The most active segment of the Lake Range fault (based on the evidence for vertical displacement) in the Holocene lies between Line D06L12 and Line D03L05, totaling a length of ~15 km. This length is used as the possible length of rupture for an earthquake event. This length gives a range of magnitudes from M6.4-M6.7 (Wells and Coppersmith, 1994; Wesnousky, 2008). For an event rupturing the entire ~41 km length of the Lake Range fault (from the northern tip of the Lake Range to Line D06L12, a magnitude M6.90-M6.95 event could ensue. An event of this magnitude would have significant effects on the Reno and Sparks metropolitan areas 64 km to the southwest.

References

Adams, K.D., compiler, 1999, Fault number 1669, Pyramid Lake fault zone, in Quaternary fault and fold database of the United States, ver. 1.0: U.S. Geological Survey Open-File Report 03-417, http://qfaults.cr.usgs.gov.

Argus, D.F., and Gordon, R.G., 1991, Current Sierra Nevada-North America motion from very long baseline interferometry; implications for the kinematics of the western United States: Geology, v. 19, p. 1085-1088.

Atwater, T., 1970, Implications of plate tectonics for the Cenozoic tectonic evolution of western North America, Geol. Soc. Am. Bulll., 81, 3513-3536.

Atwater, T., and Stock, J., 1998, Pacific–North America plate tectonics of the Neogene southwestern United States: An update: International Geology Review, v. 40, p. 375–402.

Bacon, 1983, Eruptive history of Mount Mazama and Crater Lake Caldera, Cascade Range, U.S.A: Journal of Volcanology and Geothermal Research, v. 18, p. 57-115.

Bennett, R.A., Wernicke, B.P., Niemi, N.A., Friedrich, A.M., and Davis, J. L., 2003, Contemporary strain rates in the northern Basin and Range province from GPS data: Tectonics, v. 22, 1008, doi 10.1029/2001TC001355.

Benson, L.V., Smoot, J.P., Lund, S.P., Mensing, S.A., Foit Jr., F.F., and Rye, R.O, 2013, Insights from a synthesis of old and new climate-proxy data from the Pyramid and Winnemucca lake basins for the period 48 to 11.5 cal ka, Quaternary International, v. 310, p. 62-82, doi:10.1016/j.quaint.2012.02.040.

Benson, L.V., and Mifflin, M.D., 1986, Reconnaissance bathymetry of basins occupied by Pleistocene Lake Lahontan, Nevada and California: U.S. Geological Survey Water- Resources Investigations Report 85–4262, 14 p.

Benson, L., Kashgarian, M., Rye, R., Lund, S., Paillet, F., Smoot, J., Kester, C., Mensing, S., Meko, D., Lindstrom, S., 2002. Holocene multidecadal and multicentennial droughts affecting Northern California and Nevada: Quaternary Science Reviews 21, p. 659-682.

Bonham, H.F., and Papke, K.G., 1969, Geology and mineral deposits of Washoe and Storey Counties, Nevada: Nevada Bureau of Mines and Geology Bulletin 70, 139 p.

Bosworth, W., 1985, Geometry of propagating continental rifts: Nature, v. 316, p. 625-627.

Brothers, D. S., N. W. Driscoll, G. M. Kent, A. J. Harding. J. M. Babcock and R. L. Baskin, New Constraints on the Salton Sea fault architecture and deformational history, Nature Geosciences, pp. 1-4, NGEO590, DOI:101038, 2009.

Cashman, P., and S. A., Fontaine, 2000, Stain partitioning in the northern Walker Lane, western Nevada and northeastern California, Tectonophysics, V. 326, p. 111-130, doi:10.1016/S0040-1951(00)00149-9.

Davis, J.O., 1978, Quaternary tephrochronolgy of the Lake Lahontan area, Nevada and California: Nevada Archeological Survey Research Paper, n. 7, p. 137.

dePolo, C.M., 1998, A reconnaissance technique for estimating the slip rate of normal slip faults in the Great Basin, and application to faults in Nevada, U.S.A.: Reno, [Ph.D. dissertation]: University of Nevada, Reno.

Dingler, J., Kent, G., Driscoll, N., Babcock, J., Harding, A., Seitz, G., Karlin, B., and Goldman, C., 2009, A high-resolution seismic CHIRP investigation of active normal faulting across Lake Tahoe Basin, California-Nevada: Geological Society of America Bulletin, v. 121, p. 1089-1107.

Dokka, R.K., and Travis, C. J., 1990, Role of the Eastern California Shear Zone in accommodating Pacific-North-American plate motion: Geophysical Research Letters, v. 17, n. 9, p. 1323-1326.

Driscoll, N.W., Hogg, J.R., Karner, G.D., and Christie-Blick, N., 1995, Extensional Tectonics in the Jeanne d'Arc basin: Implications for the timing of Break-up Between Grand Banks and Iberia. In Scrutton, R. A., M.S. Stoker, G.B. Shimmield, & A.W. Tudhope (eds.) The Tectonics, Sedimentation and Palaeoceanography of the North Atlantic Region Geological Society Special Publication, n. 90, p. 1-28.

Dong, S., G. Ucarkus, S. G. Wesnousky, J. Maloney, G. Kent, N. Driscoll, and R. Baskin, 2014, Strike slip faulting along the Wassuk Range of the northern Walker Lane, Geosphere 1-9, v. 10(1), doi:10.1130/GES00912.1.

Eddington, P. K., R. B. Smith, and C. Renggli, 1987, Kinematics of Basin and Range intraplate extension, in Continental Extensional Tectonics, edited by M. P. Howard, J. F. Dewey and P. L. Hancock, Geol. Soc. Spec. Pub, London 28, 371-392.

Faulds J.E., Henry, C.D., Hinz, N.H., Drakos, P.S., and Delwiche, B., 2005, Transect across the northern Walker Lane, northwest Nevada and northeast California: An incipient transform fault along the Pacific-North American plate boundary: Geological Society of America Field Guide v. 6, p. 129-150.

Flannery, J.W., and Rosendahl, B.R., 1990, The seismic stratigraphy of Lake Malawi, Africa: implications for interpreting geological processes in lacustrine rifts: Journal of African Earth Sciences, v. 10, n. 3, p. 519-548.

Gilbert, G. K., 1890, Lake Bonneville, U. S. Geological Survey Monograph 1, 438 p.

Hammond, W.C., Blewitt, G., and Kreemer, C., 2011, Block modeling of crustal deformation of the northern Walker Lane and Basin and Range from GPS Velocities: Journal of Geophysical Research, v. 116, B004402, doi: 10.1029/2010JB007817.

Kent, G.M., Babcock, J.M., Driscoll, N.W., Harding, A.J., Dingler, J.A., Seitz, G.G., Gardner, J.V., Mayer, L.A., Goldman, C.R., Heyvaert, A.C., Richards, R.C., Karlin, R., Morgan, C.W., Gayes, P.T., and Owen, L.A., 2005, 60 k.y. record of extension across the western boundary of the Basin and Range province: Estimate of slip rates from offset shoreline terraces and a catastrophic slide beneath Lake Tahoe: Geology, v. 33, n. 5, p. 356-368, doi:310.1130/G21230.21231.

McQuarrie, N., and B. P. Wernicke, 2005, An animated tectonic reconstruction of southwestern North America since 36 Ma, Geosphere, v. 1(3), p. 147-172, doi: 10:1130/GES00016.1.

Mensing, S.A., Benson, L.V., Kashgarian, M., and Lund, S., 2004, A Holocene pollen record of persistent droughts from Pyramid Lake, Nevada, USA: Quaternary Research v. 62, p. 29-38.

Oldow, J.S., 2003, Active transtensional boundary zone between the western Great Basin and Sierra Nevada block, western U.S. Cordillera: Geology, v. 31, p. 1033-1036.

Ramelli, A.R., Bell, J.W., dePolo, C.M., and Yount, J.C., 1999, Large-magnitude, late Holocene earthquakes on the Genoa Fault, west-central Nevada and eastern California, Bulletin of the Seismological Society of America, v. 89, p. 1458-1472.

Rosendahl, B.R., Kilembe, E., and Kaczmarick, K., 1992, Comparison of the Tanganyika, Malawi, Rukwa and Turkana Rift zones from analysis of seismic reflection data: Tectonophysics, v. 2213, p. 235-256.

Stewart, J.H., 1988, Tectonics of the Walker Lane belt, western Great Basin: Mesozoic and Cenozoic deformation in a zone of shear, in Ernst, W.G., ed., Metamorphism and crustal evolution of the western United States: Prentice Hall, Englewood Cliffs, New Jersey, p. 681-713.

Svarc, J. L., Savage, J.C., Prescott, W.H., and Ramelli A.R., 2002, Strain accumulation and rotation in western Nevada, 1993-2000, Journal of Geophysical Research, v. 107(B5), 10.1029/2001JB000579.

Thatcher, W., 2003, GPS constraints on the kinematics of continental deformation: International Geology Review, v. 45, p. 191– 212.

Thatcher, W., Foulger, G.R., Julian, B.R., Svarc, J.L., Quilty, E., and Bawden, G.W., 1999, Present-day deformation across the Basin and Range province, western United States: Science, v. 283, p. 1714-1718.

Turner, R., Koehler, R.D., Briggs, R.W., and Wesnousky, S.G., 2008, Paleoseismic and Slip-Rate Observations along the Honey Lake Fault Zone, Northeastern California, USA: Bulletin of the Seismological Society of America, v. 98, p. 1730-1736.

Wells, D.L., and Coppersmith, K.J., 1994, New empirical relationships among magnitude, rupture length, rupture width, rapture area, and surface displacement: Bulletin of the Seismological Society of America, v. 84, p. 974–1002.

Wesnousky, S.G., 2005a, Active faulting in the Walker Lane: Tectonics, v. 24, TC3009, p. 35.

Wesnousky, S.G., 2005b, The San Andreas and Walker Lane fault systems, western North America: transpression, transtension, cumulative slip and the structural evolution of a major transform plate boundary: Journal of Structural Geology, v. 27, p. 1505-1512.

Wesnousky, S.G., Baron, A.D., Briggs, R.W., Caskey, J.S., Kumar, S.J., and Owen, L., 2005c, Paleoseismic transect across the northern Great Basin: Journal of Geophysical Research, v. 110, B05408, doi: 10.1029/2004JB003283.

Wesnousky, S.G., 2008, Displacement and geometrical characteristics of earthquake surface ruptures: Issues and implications for seismic hazard analysis and the process of earthquake rupture: Bulletin of the Seismological Society of America, v. 98, n. 4, p. 1609–1632, doi 10.1785/0120070111.